INSIGHTS INTO THE EQUIPMENT RANDOM VIBRATION ENVIRONMENT BASED ON SIMULATIONS OF AN ACOUSTIC TEST BENCH

B. Brévart
Thales Alenia Space
26, avenue J.-F. Champollion, B.P. 1187, 31037 Toulouse Cedex 1
France

A. Pradines
Centre National d'Etudes Spatiales
18, avenue Edouard Belin, 31401 Toulouse Cedex 4
France

OVERVIEW

Random vibration tests on satellite hardware are not much representative of the mechanical stress occurring during acoustics at system level. They are often too severe and this recurrent over-testing has led to a general over-design of the on-board equipment.
Specific acoustic tests with a comprehensive instrumentation, including force cells, have been performed in order to identify and quantify the amount of over-testing on an antenna feed and an electronic unit with racked vertical PCBs [1]. Following this experimental investigation, a comprehensive analytical study of the acoustic test bench has been conducted using FEM/BEM simulations. The FE models of the feed and the electronic unit were tuned independently and an experimental modal analysis of the equipment coupled to the supporting structure was performed. This approach has led to a realistic vibro-acoustic simulation over 2000 Hz; correlation with the test results will be presented. Various simulations were then combined in order to identify for each equipment item the nature of the excitation, i.e. direct acoustics or random vibrations transmitted through the panel, with respect to the frequency range of excitation. In addition, a sensitivity analysis to the plate stiffness and to the equipment position on the panel has given new insights into the coupling phenomena taking place during the acoustic tests. The results altogether precise the origin of the H/W random vibration over-testing issue.

1. INTRODUCTION

An experimental investigation, illustrated in Figure 1, has demonstrated on an antenna feed and on an electronic unit that random vibrations are at least 3 times more severe than the acoustic test they are derived from, both for robustness (internal responses as well as I/F forces) and fatigue of the equipment [1]. To illustrate this result, Figures 2 and 3 show on one hand the PSD of an acceleration and an I/F force measured on the feed during the acoustic test, and on the other hand the envelope of the 3 accelerations (I/F forces respectively) measured during random vibrations (X, Y, Z) at a level that exactly matches the envelope of the accelerations measured on the honeycomb panel (typical of Spacebus satellite family) during the acoustic test.

Similarly, Figures 4 and 5 illustrate the PSD of an acceleration measured on the electronic unit during the acoustic test on one hand, and the envelope of the 3 accelerations measured during random vibrations (X, Y, Z) on the other hand.

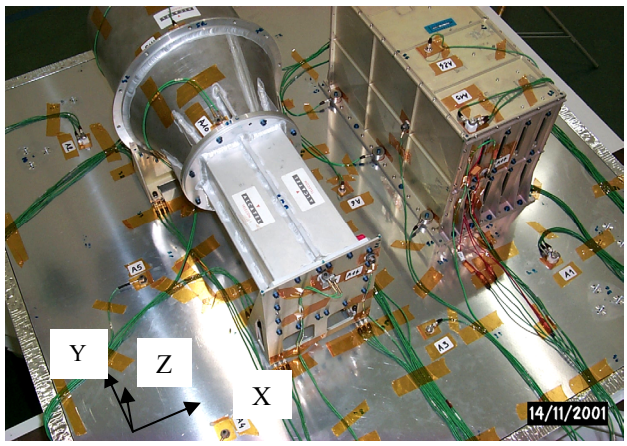

FIG 1. Acoustic test bench

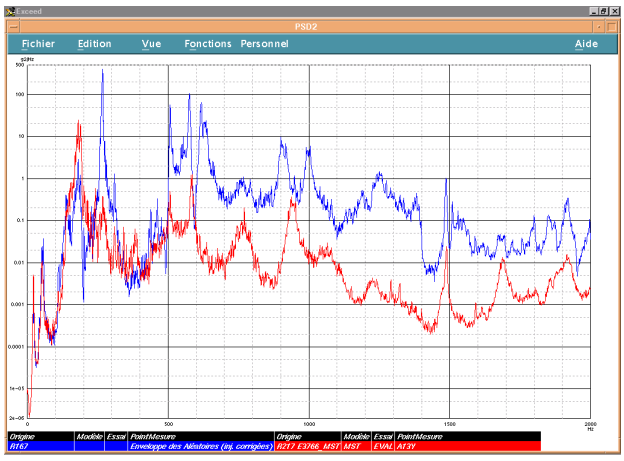

FIG 2. PSD of an acceleration measured on top of the feed, acoustics (red) versus envelope of random vibrations (blue)

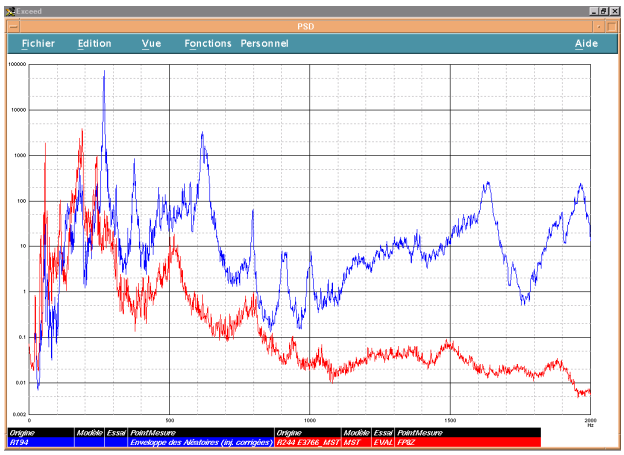

FIG 3. PSD of an out-of-plane force measured at the I/F of the feed, acoustics (red) versus envelope of random vibrations (blue)

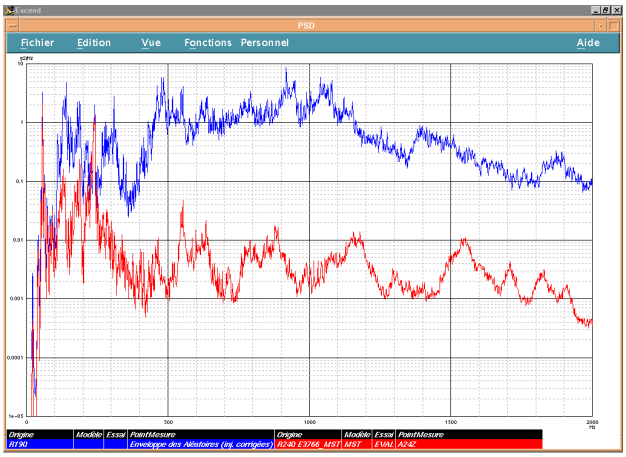

FIG 4. PSD of an acceleration on top of the electronic unit in the Z direction (⊥ to the panel), acoustics (red) versus envelope of random vibrations (blue)

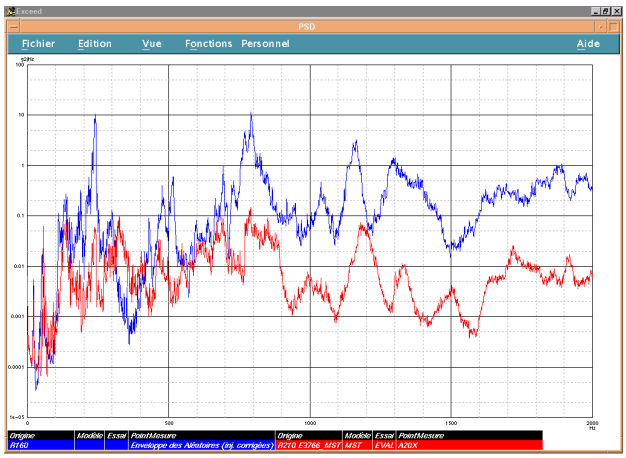

FIG 5. PSD of an acceleration on a printed circuit board of the electronic unit (⊥ to the board), acoustics (red) versus envelope of random vibrations (blue)

Two main characteristics of the random vibration over-testing issue have appeared:

– a major mismatch of the response at the equipment first resonant frequencies
– a large broadband gap at higher frequencies

The following analytical study of the acoustic test bench aims at understanding the origin of these phenomena.

2. FEM/BEM MODEL TUNING

The FE models of the feed and the electronic unit were first tuned to meet random vibration responses with rigid boundary conditions. In Figure 6 is recalled the instrumentation of the equipment.

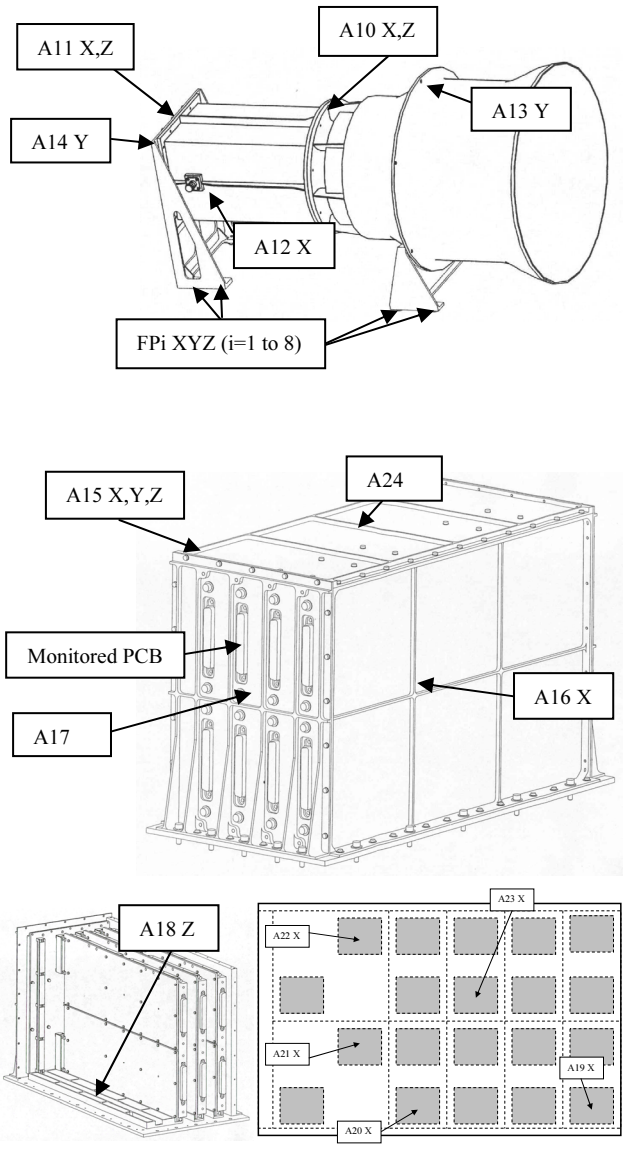

FIG 6. Instrumentation of the equipment

Figures 7 and 8 illustrate the results obtained on the feed with ξ=1% damping. Figures 9 and 10 illustrate the results achieved on the electronic unit (case and printed circuit board) with 3% damping on the printed circuit boards and 1.5% on the structure.
An experimental modal analysis of the equipment coupled to the supporting structure was performed. At the exception of one mode that the model did not exhibit, a good match of the eigenfrequencies up to 500 Hz was

achieved (see Table 1). Corresponding mode shapes were verified, as illustrated by Figure 11 and 12.

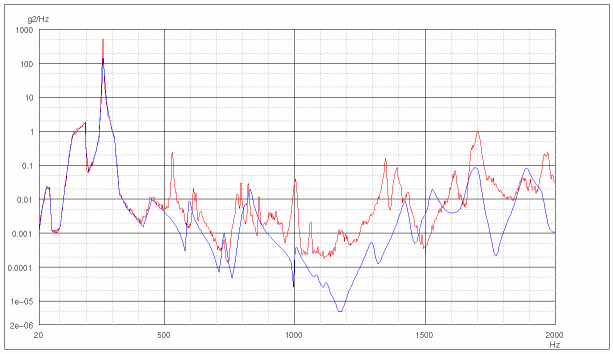

FIG 7. Random vibration excitation of the feed along Y axis. Measured (red) and predicted (blue) acceleration PSD at location A14Y

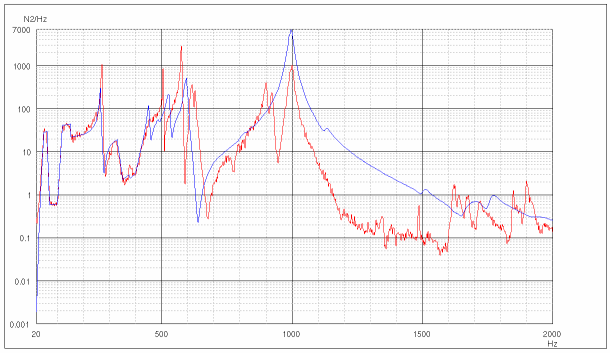

FIG 8. Random vibration excitation of the feed along Z axis. Measured (red) and predicted (blue) I/F load PSD at location FP1Z

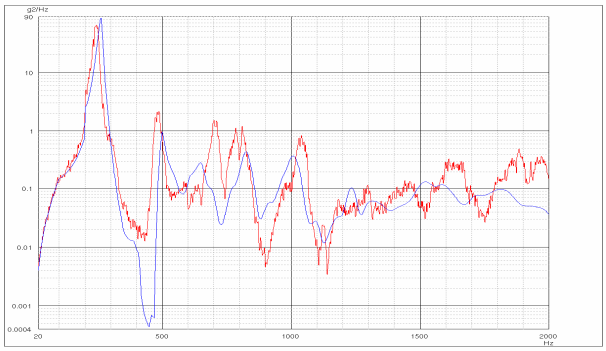

FIG 9. Random vibration excitation of the electronic unit along X axis. Measured (red) and predicted (blue) acceleration PSD at location A23X

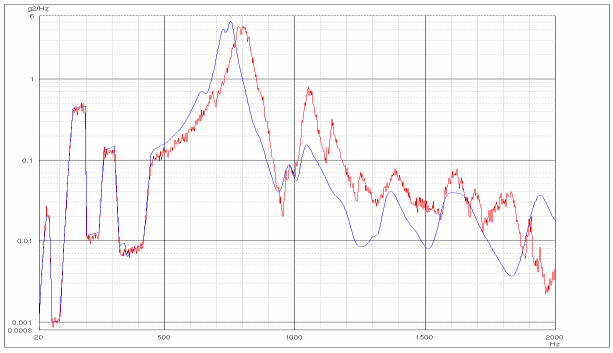

FIG 10. Random vibration excitation of the electronic unit along Y axis. Measured (red) and predicted (blue) acceleration PSD at location A15Y

Calculated eigenfrequencies (Hz)	Measured eigenfrequencies (Hz)
25.69	19.9
25.93	26.03
57.99	58.52
68.29	*Could not be identified because of experimental mesh choice*
117.29	121.29
146.55	153.11
152.84	169.89
Not found	186.73
166.00	196.62
237.45	221.25
248.22	257.21
290.30	313.61
380.74	352.81
443.38	409.46

TAB 1. Calculated and measured eigenfrequencies of the acoustic test bench

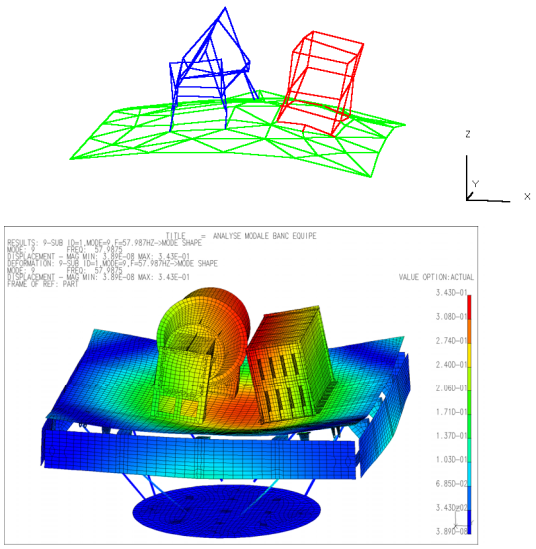

FIG 11. Experimental and calculated mode shapes at 59 and 58 Hz respectively

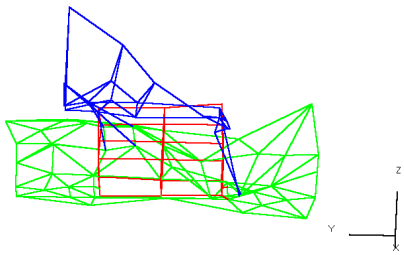

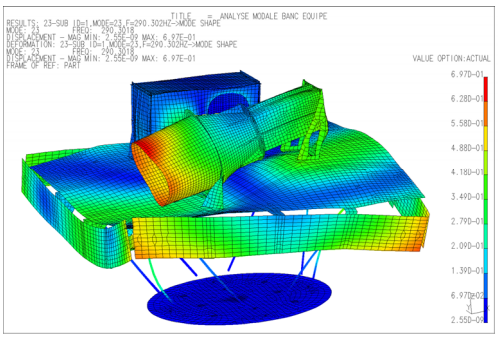

FIG 12. Experimental and calculated mode shape at 290 Hz and 314 Hz respectively

The acoustic simulations have been performed in the frequency domain using the boundary element method (RAYON software). The diffuse acoustic field was simulated by applying 26 uncorrelated plane waves. The acoustic mesh is illustrated on Figure 13 and includes the four printed circuit boards inside the electronic unit. The largest boundary element is smaller than a quarter of the acoustic wavelength at 2000 Hz. Note that a smaller mesh (number of elements x 4) did not much affect the results. The applied damping factor was uniform over the frequency range. Its value resulted from a compromise to meet the largest number of measurements. Figure 14 illustrates the effects of the damping factor. The first one is the classic amplification of the low frequency resonances. At higher frequencies, the modal density is such that a lower damping results in a broadband elevation of the responses.
Best overall results were obtained with a damping factor of 1% (best match for both the feed and the sandwich panel) even though it overestimates the low frequency response of the printed circuit boards in the electronic unit.

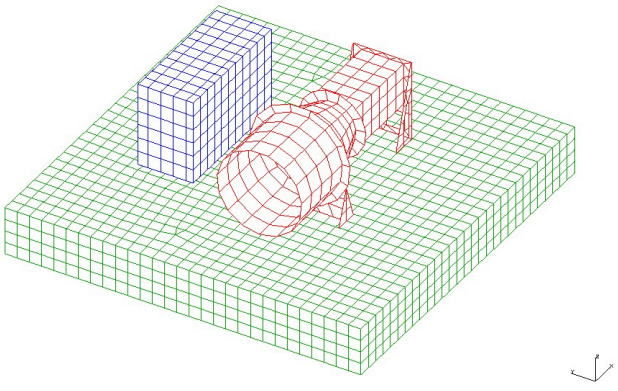

FIG 13. Acoustic mesh of the test bench

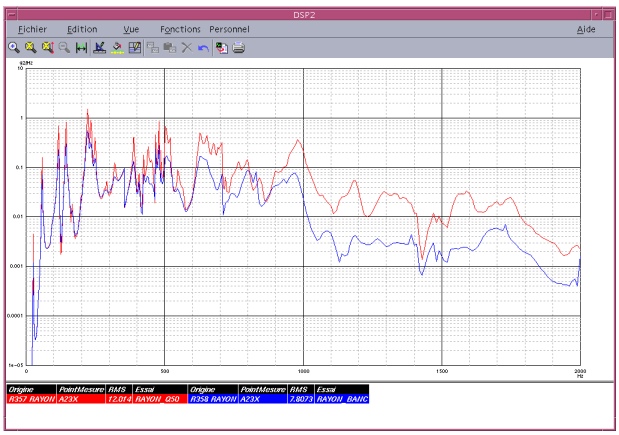

FIG 14. Calculated response of the electronic unit PCB with 2 different damping factors (ξ=1 and 2 %)

Figures 15 and 16 illustrate the results obtained in plane and out of the plane of the supporting structure w.r.t. the associated measurements. Good correlation is achieved up to 1200 Hz (DSP peak value and overall shape) with RMS values differing by less than 30%. Figure 17 shows the superposition of calculated and measured responses on the feed. Once again, good correlation is achieved up to 1200 Hz. Figure 18 shows the superposition of calculated and measured loads (X,Y,Z) at the interface between the feed and the supporting structure. Very good overall correlation is achieved on the highest loads (Y,Z) with RMS values differing by less than 30%. Figure 19 shows the superposition of calculated and measured accelerations on the electronic unit. The damping is obviously under estimated (by a factor 3) on the fundamental mode of the equipment at 146 Hz and on the printed circuit boards (all modes). As a result, RMS values on the PCB are overestimated, up to 100%, but the overall PSD shape of the accelerations is respected. In addition, the missing mode at 187 Hz in the model appears to be coupling the supporting panel the electronic unit along Y axis and generates a discrepancy on the unit response at this frequency.

Finally, despite the damping issue (inhomogeneous over the system), it appears that the vibro-acoustic simulation is very realistic over a large frequency range. Even though the discrepancies are more significant above 1200 Hz or so, it is believed that the conclusions of this study in this frequency range should remain valid and all simulations were thus conducted up to 2000 Hz.

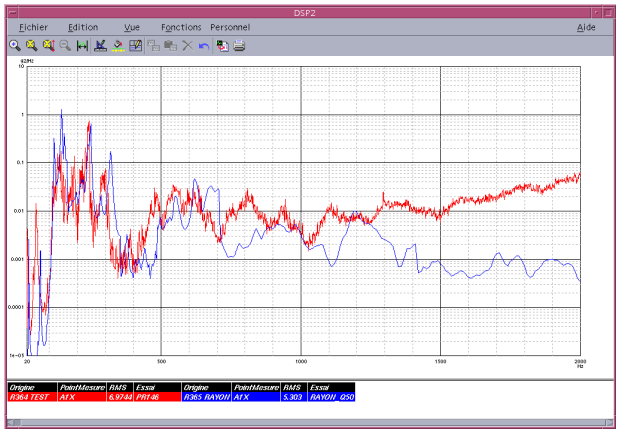

FIG 15. Calculated and measured acoustic responses of the test bench, acceleration on the supporting panel in plane (A1X)

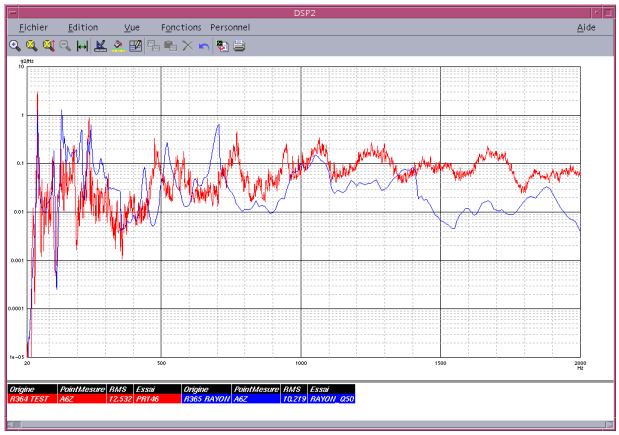

FIG 16. Calculated and measured acoustic responses of the test bench, acceleration on the supporting panel out of plane (A6Z)

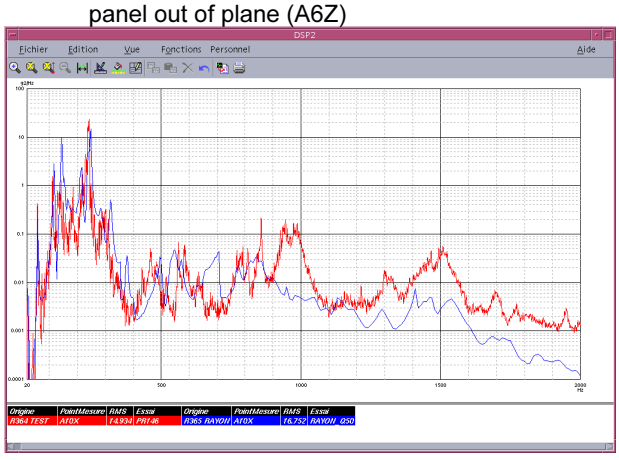

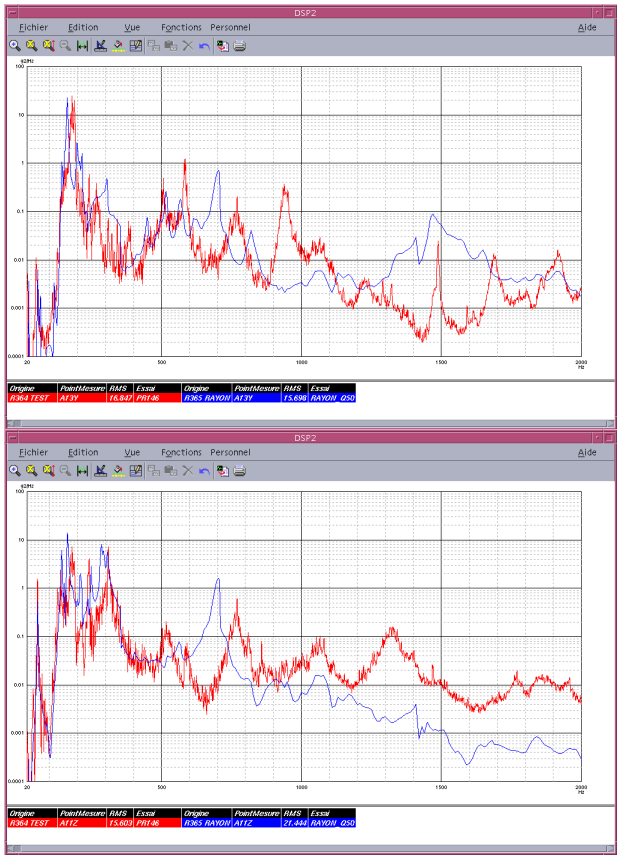

FIG 17. Calculated and measured acoustic responses of the test bench, accelerations on the feed

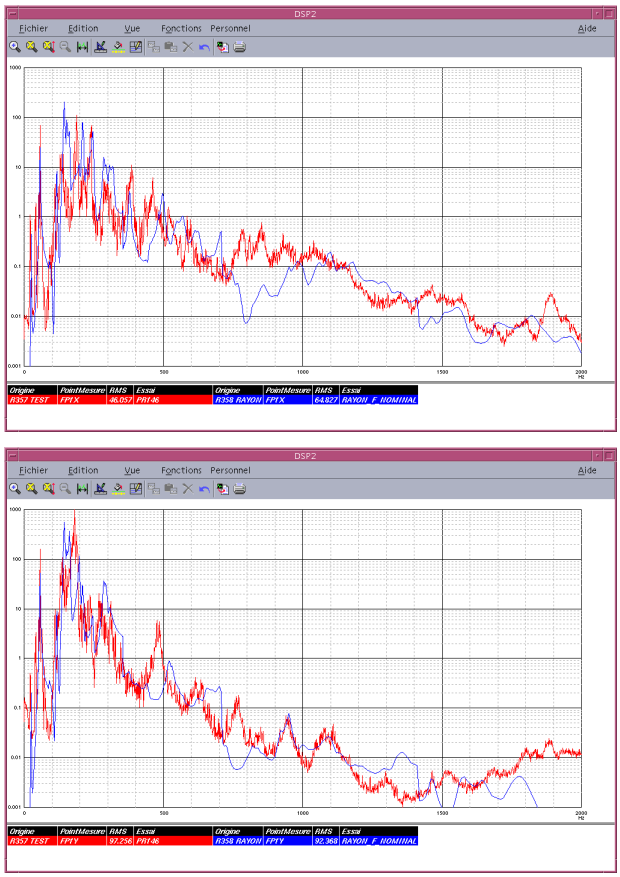

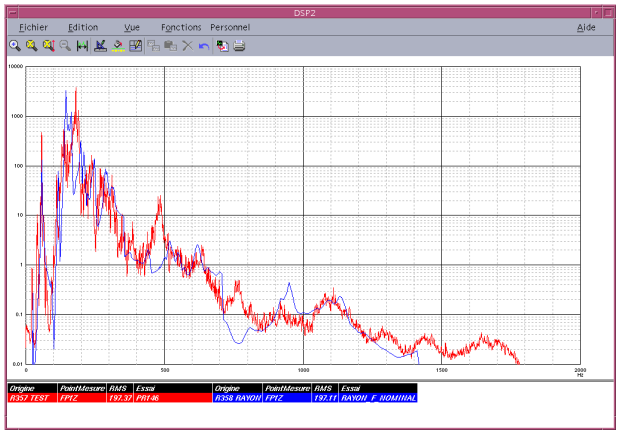

FIG 18. Calculated and measured acoustic responses of the test bench, loads at the feed interface

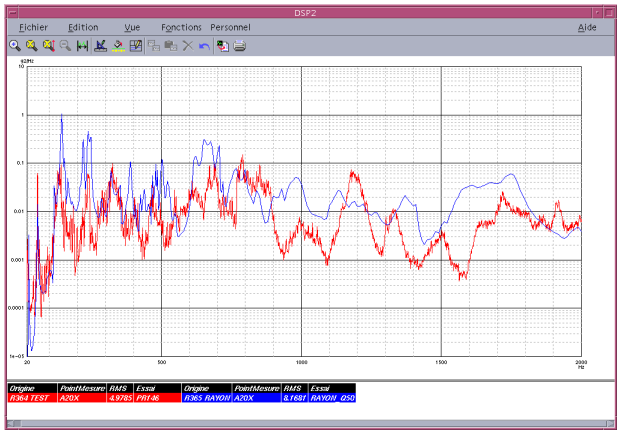

FIG 19. Calculated and measured acoustic responses of the test bench, accelerations on the electronic unit

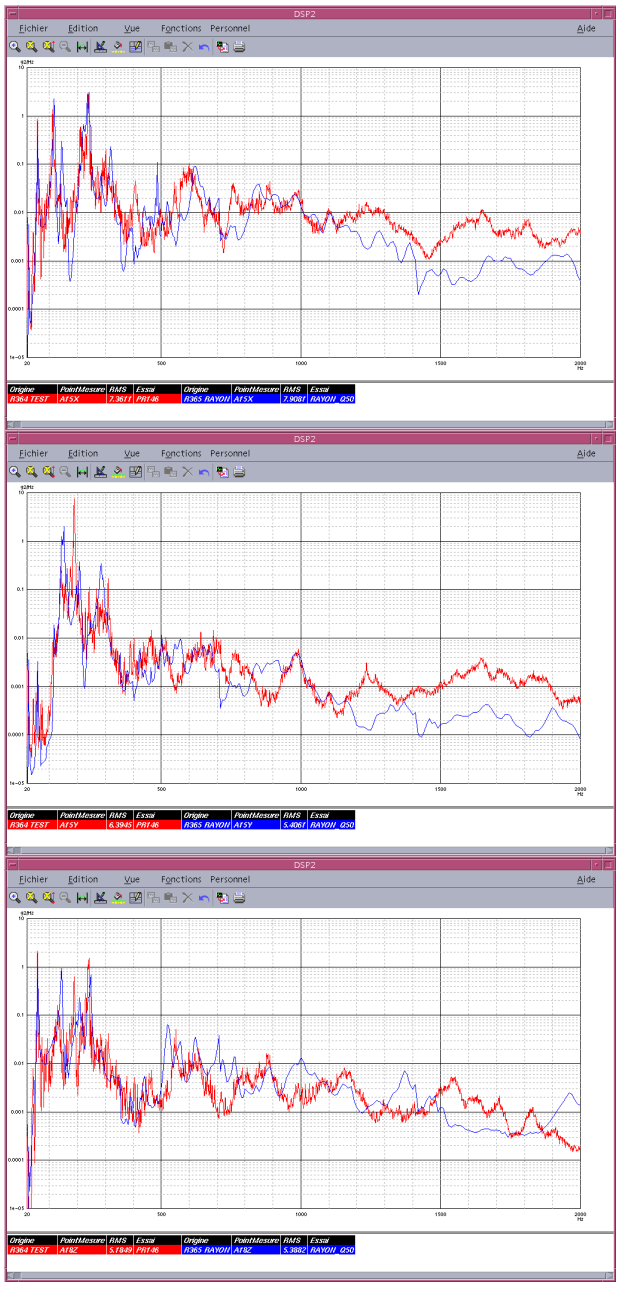

3. STRUCTURAL EXCITATION OF THE EQUIPMENT

Keeping in mind that the final objective of the present study is to better understand the major difference between a random vibration excitation, with rigid boundary conditions of the equipment, and its real acoustic excitation on a satellite panel, the investigation has first focussed on the random vibration excitation of the equipment through the supporting structure. In plane random acceleration along X or Y axis has thus been applied to the panel and the equipment response in the same direction has been analyzed. In addition various configurations derived from the initial system have been investigated, such as:

- various stiffness of the supporting panel (low, high, w.r.t. Spacebus honeycomb panel)
- various positions of the electronic unit on the panel (initial, close to the edge)

As illustrated by Figure 20, it appears that the RMS responses of the feed are raised on the panel (up to 100%) due to a large quasi-static behaviour of the equipment below 200 Hz that carries all the I/F load (Fig. 21). On the panel, the fundamental modes of the feed are filtered but strong coupling phenomena appear at higher frequencies.

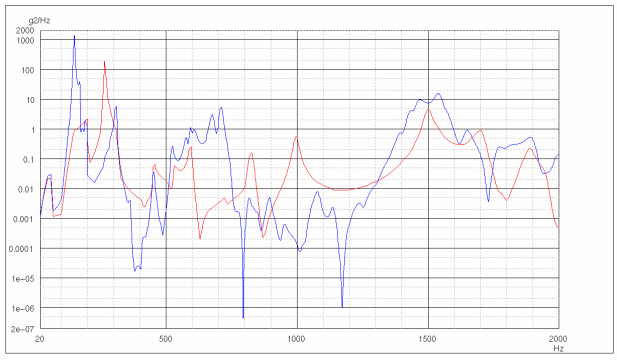

FIG 20. Random vibration response (A13Y) of the feed along Y axis – Rigid interface (red), on the test bench (blue)

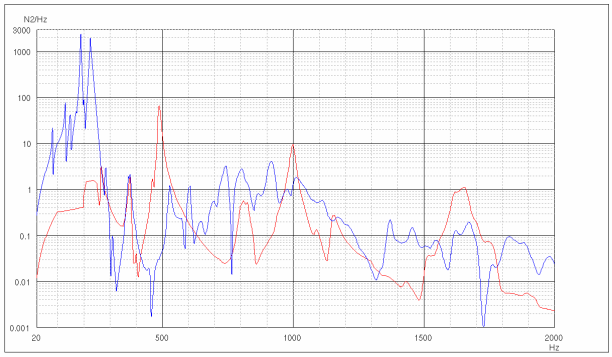

FIG 21. Random vibration load (FP6X) at the I/F of the feed along X axis – Rigid interface (red), on the test bench (blue)

Similar behaviour is observed on the electronic unit but, unlike the feed, RMS levels on top of the unit (Fig. 22) and on the printed circuit board along X axis (normal direction to the board) are lower on the panel (up to 30%). The opposite is observed along Y axis (Fig. 23), with almost no filtering of the fundamental mode of the equipment and a RMS level that is doubled on the panel.
In addition, Figure 22 shows that the high frequency response (above 1000 Hz) of the electronic unit is highly increased when the unit is moved to the edge of the panel. Figure 23 exhibits a strong amplification of the unit response along Y axis around 500 Hz when the stiffness of the panel is lowered.

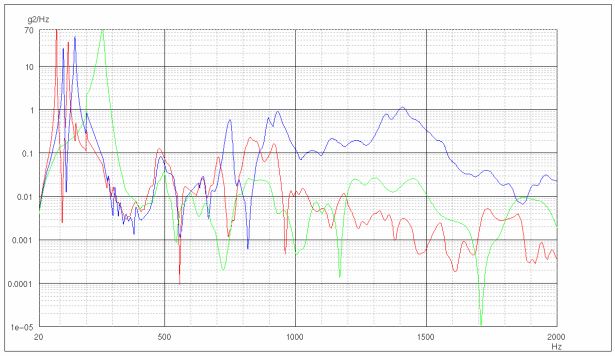

FIG 22. Random vibration response (A15X) on top of electronic unit along X axis – Rigid interface (green), initial position (red) and unit on edge of panel (blue)

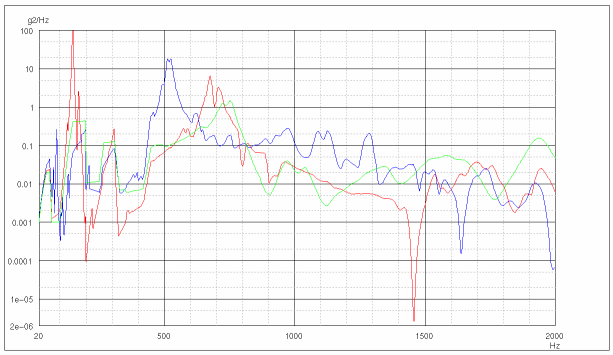

FIG 23. Random vibration response (A17Y) of the electronic unit along Y axis – Rigid I/F (green), initial stiffness (red) and low stiffness panel (blue)

4. SENSITIVITY OF THE VIBRO-ACOUSTIC ANALYSIS

4.1. To the panel stiffness

In acoustics, when lowering the stiffness of the supporting panel, in plane and out of plane responses of the panel itself (Fig. 24, 25) increase considerably for frequencies above 350 H. On the equipment however, in this frequency range, the effect is barely noticeable at all measurement points, as illustrated by Figure 25 to 28. Note in particular on Figure 27 that the large response amplification predicted around 500 Hz by the structural excitation of the electronic unit (Fig. 14) did not occur.

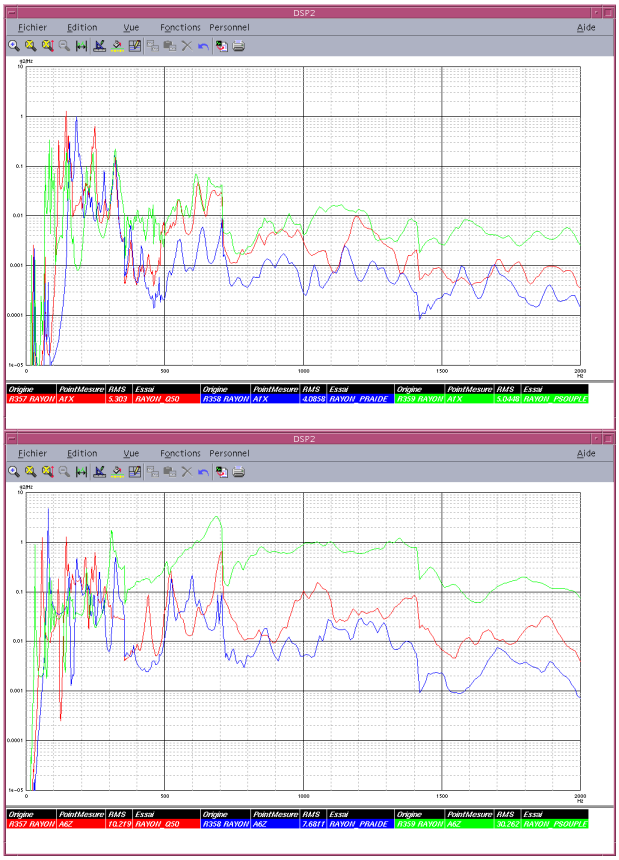

FIG 24. Calculated acoustic responses of the test bench panel – Initial stiffness (red), low stiffness (green) and high stiffness panel (blue)

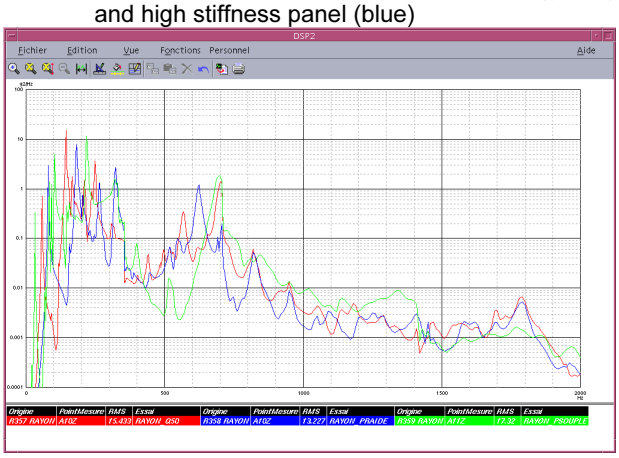

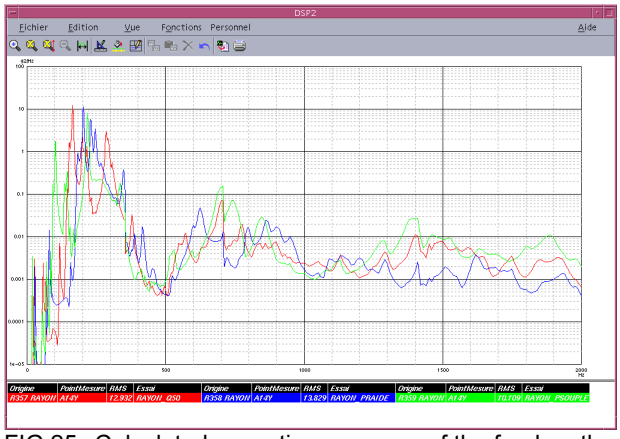

FIG 25. Calculated acoustic responses of the feed on the test bench– Initial stiffness (red), low stiffness (green) and high stiffness panel (blue)

As expected, at low frequencies, it appears that the largest loads (Y and Z axis) at the interface of the feed increase with the stiffness of the panel (Fig. 26), and they are spread over a larger frequency range. These effects are similar and even more noticeable at the interface of the electronic unit (Fig. 28)

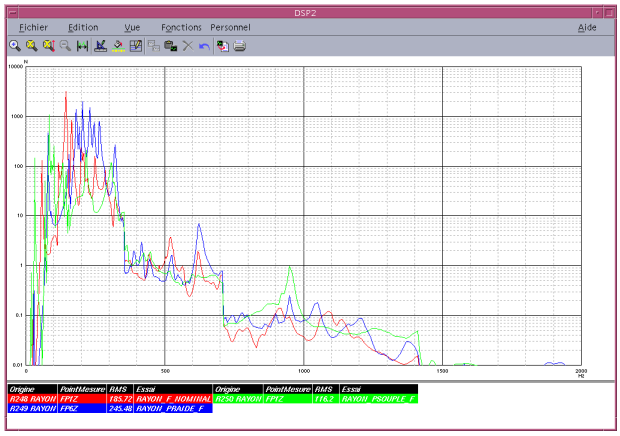

FIG 26. Calculated acoustic load at the I/F of the feed on the test bench – Initial stiffness (red), low stiffness (green) and high stiffness panel (blue)

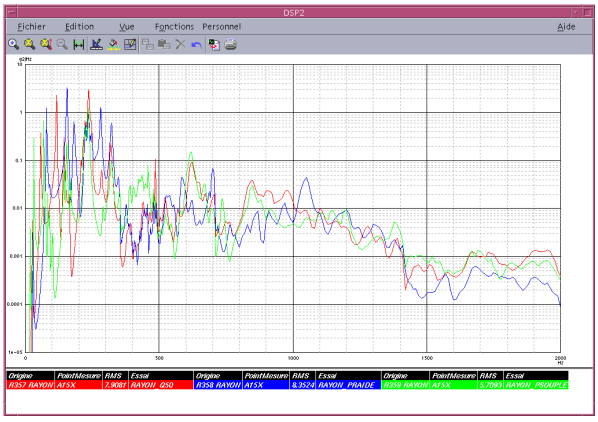

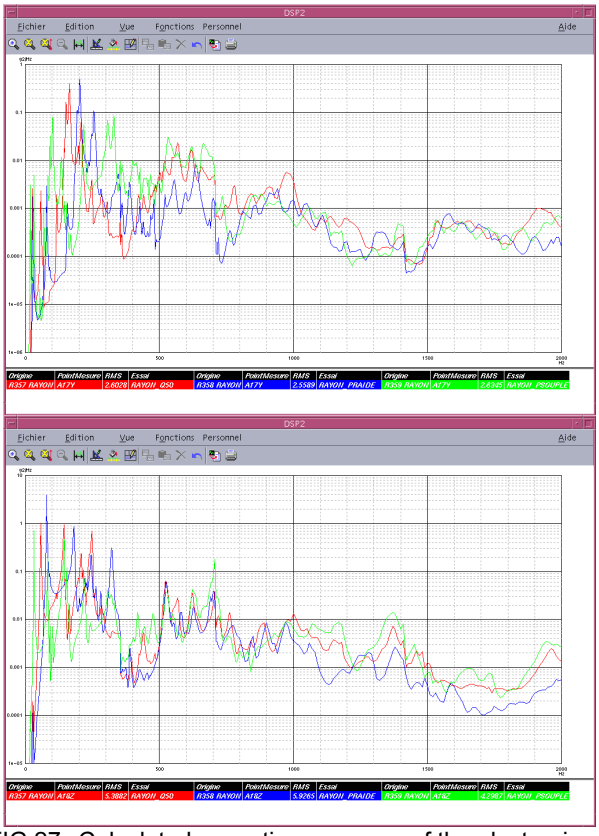

FIG 27. Calculated acoustic responses of the electronic unit on the test bench – Initial stiffness (red), low stiffness (green) and high stiffness panel (blue)

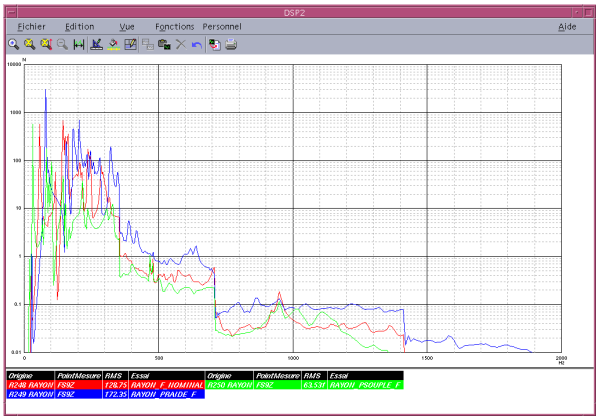

FIG 28. Calculated acoustic load at the I/F of the elec. unit on the test bench – Initial stiffness (red), low stiffness (green) and high stiffness panel (blue)

4.2. To the equipment position

When changing the position of the electronic unit on the supporting panel, from the initial position to the edge, the in plane acceleration of the panel is almost unchanged at high frequencies as appear in Figure 29. And so is the response on top of the electronic unit along X axis (Fig. 30). This result contrasts significantly with the result of Figure 22 that predicts that the response of the unit to a structural excitation along X axis should be largely amplified above 1000 Hz when the unit is moved to the edge of the panel.
On the other hand, RMS accelerations on the PCB and loads (X, Y, Z) at the I/F of the unit slightly increase (up to

20%) when the equipment is moved to the edge, because of low frequency behaviour (<800 Hz).

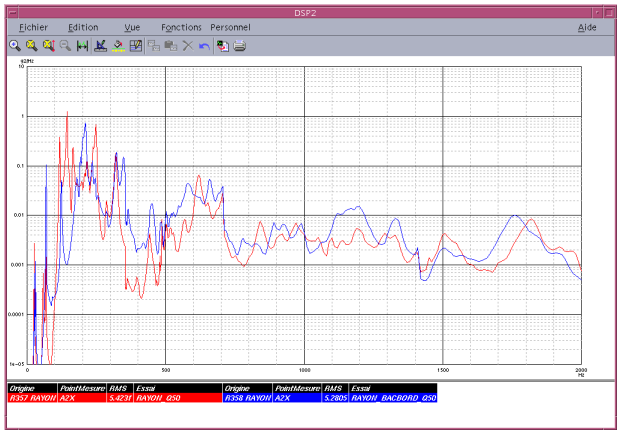

FIG 29. Calculated acoustic response of the test bench panel – Initial position of the unit (red), electronic unit on the edge of the panel (blue)

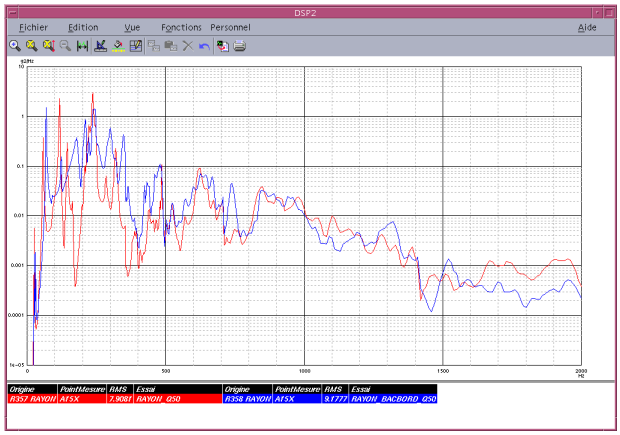

FIG 30. Calculated acoustic response of the electronic unit on the test bench panel – Initial position of the unit (red), unit on the edge of the panel (blue)

5. VIBRATION TRANSMISSION PATHS

Acoustic simulations of the antenna feed alone and of the electronic unit alone have allowed to identify which simple boundary conditions best meet the real interface conditions of the equipment on the panel. It appears that “free” boundary conditions best fit the antenna feed responses over a large frequency range. “Clamped” boundary conditions best fit the responses of the electronic unit.

Then, in order to identify the vibration transmission paths of the acoustic excitation w.r.t. the frequency, three calculated DSP curves were superimposed for various response locations on the equipment:

- the acoustic response of the equipment on the test bench
- the acoustic response of the equipment alone
- the random vibration response of the equipment to an in plane structural excitation of the panel at the exact level obtained by the acoustic load case on the test bench

Note that, if in plane and out of plane responses of the supporting panel are coherent (i.e. linked by a valid transfer function), then the out of plane excitation of the equipment is implicit in the third load case.

5.1. On the antenna feed

Three frequency zones can be identified. The first one, from 0 to 350 Hz, is largely dominated by the coherent random vibration excitation of the interface. The vibration transmission path in the second zone, from 350 to 700 Hz, is not clearly defined. In this range, depending on the measurement location, the response may be alternatively due to direct acoustics (A12X, i.e. on the flange) or to the structural excitation. From 700 Hz to 2000 Hz, the response of the feed is directly due to the acoustic excitation at most locations. At A11 location, i.e. close to the I/F, the feed is very stiff along X axis and the structural excitation dominates the response over the whole frequency range.

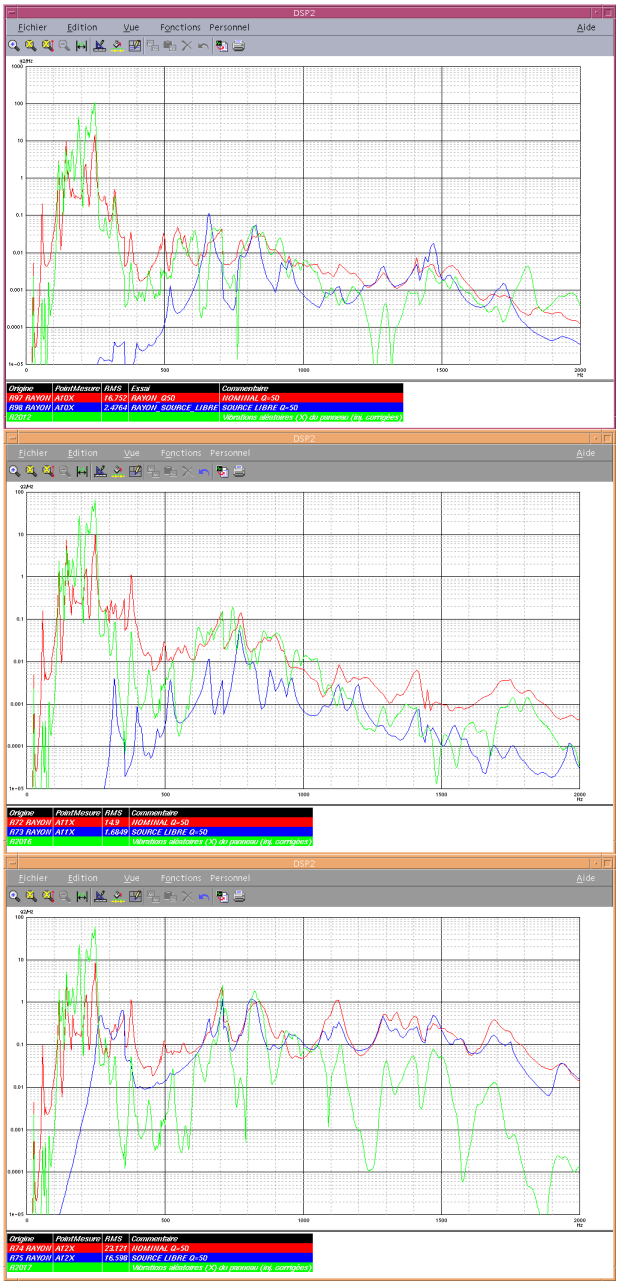

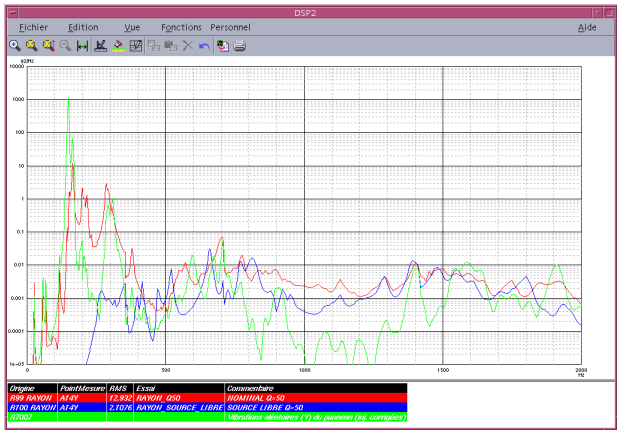

FIG 31. Calculated responses of the antenna feed – Acoustics on the test bench (red), acoustics of the feed alone (blue), structural excitation (green)

5.2. On the electronic unit

Four frequency zones can be identified. The first one, from 0 to 350 Hz, is largely dominated by the coherent random vibration excitation of the interface. In the second zone, from 350 to 550 Hz, the response is mostly due to the direct acoustic excitation of the unit. From 550 to 950 Hz, the responses are once again dominated by the structural excitation. From 950 Hz to 2000 Hz, the response of the unit in the Y direction remains controlled by the structural path but it appears that the responses in the X direction, on the printed circuit board in particular, are not covered by any of the two load cases. The origin of the responses in this frequency range must thus be found in the diffuse nature of the vibration field (Z axis).

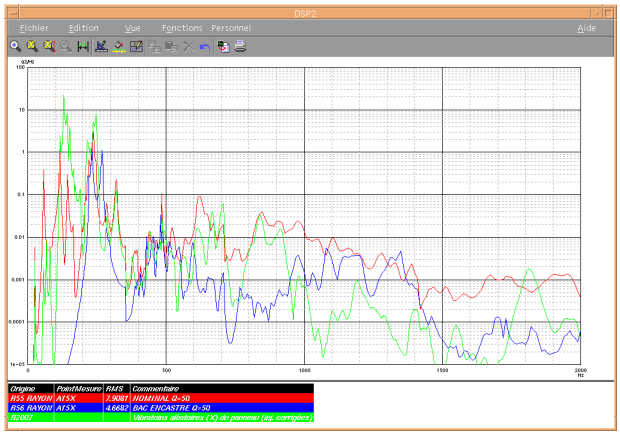

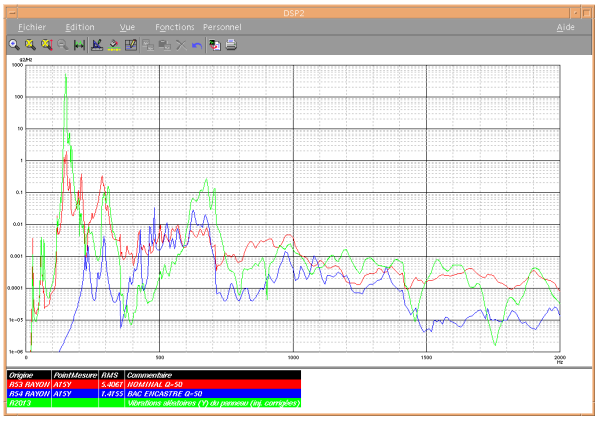

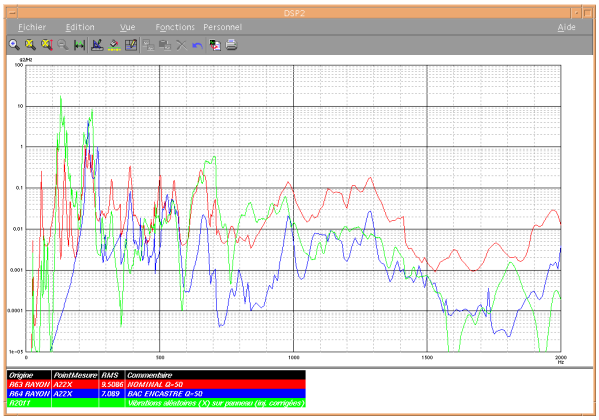

FIG 32. Calculated responses of the electronic unit – Acoustics on the test bench (red), acoustics of the unit alone (blue), structural excitation (green)

Figure 33 shows on one hand the envelope of the nine calculated accelerations of the panel at the origin of the random vibration specification (along Z axis) and on the other hand the envelope of the 20 accelerations at the true interface locations of the electronic unit. It appears that the mass of the equipment on the panel is at the origin of 10 to 15 dB local filtering (mass law) from 150 to 2000 Hz.
In fact, because the unit is much stiffer than the panel, the 20 accelerations are very homogeneous, and probably coherent. Applying this acceleration field to the unit (with rigid boundary condition), the responses of the PCB well match the acoustic responses on the test bench from 1000 to 2000 Hz, as illustrated on Figure 34.

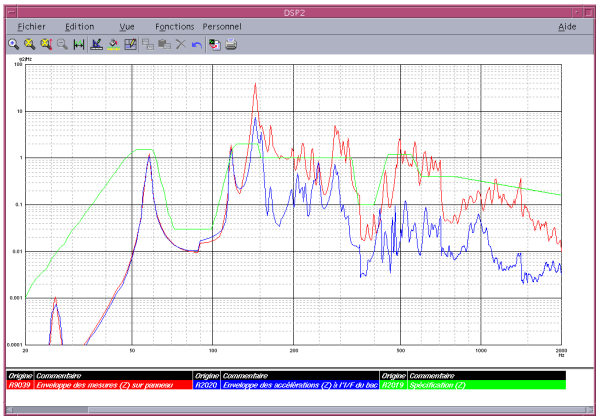

FIG 33. Envelope of the 9 calculated accelerations (A1Z-A9Z) on the panel (red) and envelope of the 20 accelerations at the I/F of the electronic unit

Because the electronic unit materializes a strong rupture of impedance with the panel, all accelerations along Z axis on the unit are filtered over the whole frequency range with respect to the true acceleration field at the interface, as illustrated on Figure 35.

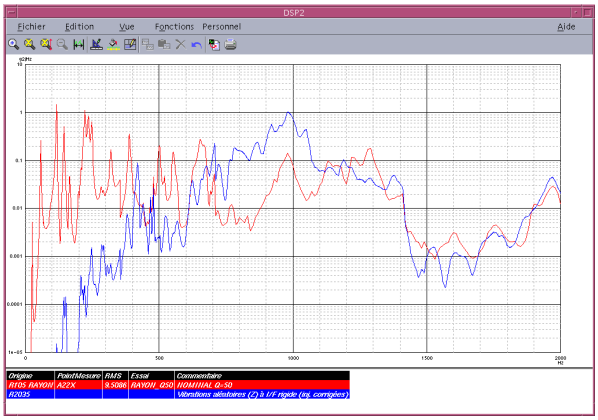

FIG 34. Calculated response (A22X) of the electronic unit – Acoustics on the test bench (red), random vibrations with rigid bc along Z axis (blue)

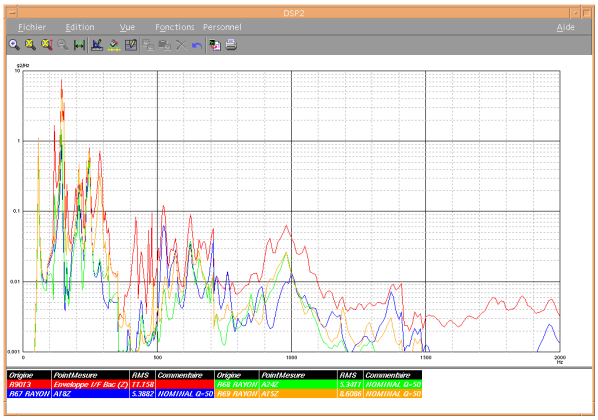

FIG 35. Calculated responses of the unit in Z direction w.r.t. the interface acceleration field (red)

6. CONCLUSIONS

The nature of the acoustic excitation of a payload equipment mounted on a test bench, whose dynamic behaviour is representative of a satellite panel, has been analyzed. Various vibration transmission paths have been identified over the frequency range of interest.
The stiffness of the panel and the position of the unit on the panel only affect the low frequency responses of the equipment. At high frequencies, the antenna feed (large light structure) is directly controlled by the acoustic field and the acceleration of the heavy electronic unit is mostly controlled by its own mass (mass law). The real acceleration level at the true interface of the equipment is over-estimated by nearby measurements, which explains the broadband gap that partially characterizes the over-testing issue [1].

REFERENCES

[1] Brévart B., Pradines A. 2002 *European Conference on Spacecraft Structures, Materials, and Mechanical Testing*, Toulouse, F, Dec. 2002. Comparison of Satellite Equipment Responses Induced by Acoustic and Random Vibration Tests.